

Supporting Information for

**Highly symmetric Ln(III) boron-containing macrocycles as bright
fluorophores for living cell imaging**

Zhenhua Zhu,^{1,2,‡} Guo-Qing Jin,^{3,‡} Jinjiang Wu,^{1,4} Xu Ying,^{1,4} Chen Zhao,^{1,4} Jun-Long Zhang^{3,*} and Jinkui Tang^{1,4,*}

¹State Key Laboratory of Rare Earth Resource Utilization, Changchun Institute of Applied Chemistry, Chinese Academy of Sciences, Changchun 130022, P.R. China;

²University of Chinese Academy of Sciences, Beijing 100049, P.R. China;

³Beijing National Laboratory for Molecular Sciences, College of Chemistry and Molecular Engineering, Peking University, Beijing, 100871, P.R. China;

⁴University of Science and Technology of China, Hefei 230026.

*Corresponding authors. Email: tang@ciac.ac.cn and zhangjunlong@pku.edu.cn

‡Equally contributed to this work.

Contents

1. General information	S2
2. Synthesis of Ln-B-Ph₃PO and Ln-B-AnPh₃PO	S3
3. Single-crystal X-ray crystallography	S4-S10
4. TGA and magnetic measurements	S11-S12
5. Photophysical properties	S13-S19
6. Living cell imaging	S20
7. References	S21

1. General information

Toluene used for synthesis was freshly distilled prior to use and stored over activated 4 Å molecular sieves in the Ar filled glovebox. Ph₃PO and Catecholborane (HBCat) were purchased from J&K Chemical Co. and used as received. Anhydrous LnCl₃, Ln[N(TMS)₂]₃ and AnPh₃PO were prepared according to literature procedures.¹⁻³ X-ray diffraction data of **Ln-B-Ph₃PO** and **Dy-B-Cy₃PO** were collected on a Bruker Apex II CCD diffractometer equipped with an Oxford low temperature apparatus using MoK α radiation ($\lambda = 0.71073 \text{ \AA}$). The structure was solved in Olex2 with SHELXT using intrinsic phasing and were refined with SHELXL using least squares minimization.⁴ The crystal data have been deposited at the Cambridge Structural Database (CCDC-1990956, 2165282, 2165283, 2165423), which can be obtained free of charge via www.ccdc.cam.ac.uk/data_request/cif. PXRD data were collected on a Bruker D8 advance X-ray diffractometer using Cu K α radiation ($\lambda = 1.54184 \text{ \AA}$). TGA were performed on a Netzsch STA 449F3 analyzer. Elemental analyses (C, H, N) were performed on a Perkin-Elmer 2400 analyzer. The magnetic properties were explored using a Quantum Design MPMS XL-7 SQUID magnetometer. Variable-temperature dc magnetic susceptibility was performed in the temperature range 1.9-300 K under a 1000 Oe dc field while ac magnetic susceptibility was collected under a zero dc field with an oscillating field of 3 Oe. The polycrystalline or powder samples were sealed in a polyethylene membrane in a glass tube with an inert atmosphere before test. The experimental magnetic data are corrected for the diamagnetism estimated from Pascal's constants and sample holder calibration.⁵ Solid-state and solution UV-vis spectra were recorded in different modes on a Hitachi U-4100 UV-vis-NIR spectrophotometer. The photoluminescence excitation and photoluminescence emission spectra were collected using an Edinburgh Instruments FLSP-920 fluorescence spectrometer equipped with a 450 W xenon lamp as the excitation source at room temperature. The luminescence decay lifetimes were analyzed with a Lecroy Wave Runner 6100 digital oscilloscope (1 GHz) using a tunable laser (pulse width 4 ns, gate 50 ns) as the excitation (Continuum Sunlite OPO). The overall luminescence quantum yields were determined by an integrating sphere on a FLS1000 instrument.

2. Synthesis of Ln-B-Ph₃PO and Ln-B-AnPh₃PO

Synthesis of Dy-B-Ph₃PO:

Dy[N(SiMe₃)₂]₃ (0.3 mmol, 0.195 g), HBCat (2.7 mmol, 0.324 g), Ph₃PO (0.6 mmol, 0.167 g) and 10 mL toluene were added to a dried Schlenk tube equipped with a stirrer bar in the glovebox. The tube was sealed and the mixture was stirred at 90 °C for 24 h. Then, it was filtered and allowed to stand undisturbed at room temperature for several days to yield colorless bulk crystals in the shape of regular hexagon (yield: 61% based on Dy). Elemental analysis / %, found (calculated) for **Dy-B-Ph₃PO**: C 61.55 (61.77); H 3.81 (3.89).

Synthesis of Dy-B-Cy₃PO:

The synthesis procedures were similar to that of **Dy-B-Ph₃PO**, except using Cy₃PO as starting materials (yield: 43% based on Dy). Elemental analysis / %, found (calculated) for **Dy-B-Cy₃PO**: C 60.26 (60.43); H 6.29 (6.34).

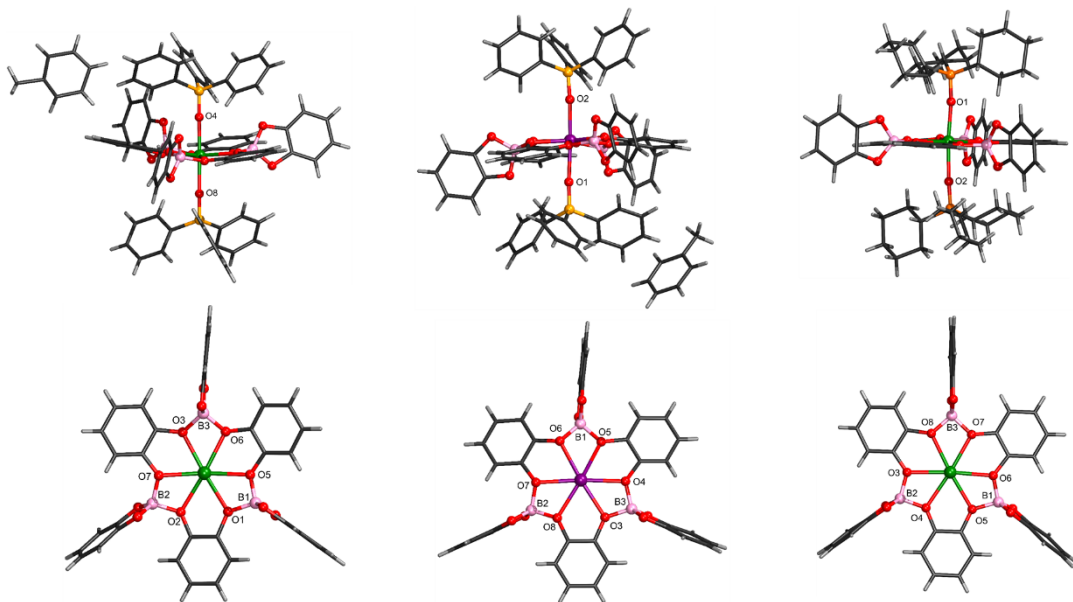
Synthesis of Yb-B-Ph₃PO and Gd-B-Ph₃PO:

The synthesis procedures of these two complexes were similar to that of **Dy-B-Ph₃PO**, except using Yb[N(SiMe₃)₂]₃ and Gd[N(SiMe₃)₂]₃ as starting materials (yield: 73% for **Yb-B-Ph₃PO** and 56% for **Gd-B-Ph₃PO** based on Ln). Elemental analysis / %, found (calculated) for **Yb-B-Ph₃PO**: C 61.07 (61.30); H 3.73 (3.86); **Gd-B-Ph₃PO**: C 61.26 (62.00); H 3.93 (3.90).

Synthesis of Yb-B-AnPh₃PO and Gd-B-AnPh₃PO:

The synthesis procedures of these two complexes were similar to that of **Dy-B-Ph₃PO**, except using Yb[N(SiMe₃)₂]₃ and Gd[N(SiMe₃)₂]₃ as well as AnPh₃PO as starting materials (yield: 49% for **Yb-B-AnPh₃PO** and 57% for **Gd-B-AnPh₃PO** based on Ln). Elemental analysis / %, found (calculated) for **Yb-B-AnPh₃PO**: C 67.96 (68.13); H 3.93 (4.00); **Gd-B-AnPh₃PO**: C 68.67 (68.74); H 4.08 (4.04).

3. Single-crystal X-ray crystallography



Figs. S1 Molecular structures and equatorial plane for **Yb-B-Ph₃PO**, **Gd-B-Ph₃PO** and **Dy-B-Cy₃PO** from left to right.

Table S1. Crystal Data and Structure Refinement for **Dy-B-Ph₃PO** and **Gd-B-Ph₃PO**.

Compound reference	Dy-B-Ph₃PO	Gd-B-Ph₃PO
Chemical formula	C ₇₂ H ₅₄ B ₃ DyO ₁₄ P ₂	C ₇₂ H ₅₄ B ₃ GdO ₁₄ P ₂ ·C ₇ H ₈
Formula Mass	1400.03	1486.90
Temperature (K)	180.0	180.0
Crystal system	trigonal	triclinic
Space group	<i>R</i> -3	<i>P</i> -1
<i>a</i> (Å)	18.3591(6)	14.2030(5)
<i>b</i> (Å)	18.3591(6)	16.7770(6)
<i>c</i> (Å)	33.5988(13)	18.4196(7)
α (°)	90.000	79.004(2)
β (°)	90.000	69.4470(10)
γ (°)	120.000	71.9180(10)
Unit cell volume (Å ³)	9807.5(7)	3890.2(2)
<i>Z</i>	6	2
ρ_{calc} (g/cm ³)	1.422	1.269
μ / mm ⁻¹	1.258	0.953
<i>F</i> (000)	4254	1514.0
Radiation	MoK α (λ = 0.71073)	MoK α (λ = 0.71073)
Reflections collected	22875	70478
Independent reflections	3356	14212
<i>R</i> _{int}	0.0380	0.0486
GOF on <i>F</i> ²	1.043	1.080
<i>R</i> ₁ (<i>I</i> ≥ 2σ(<i>I</i>))	0.0223	0.0250
<i>wR</i> ₂ (all data)	0.0557	0.0640
CCDC number	1990956	2165282

Table S2. Crystal Data and Structure Refinement for **Yb-B-Ph₃PO** and **Dy-B-Cy₃PO**.

Compound reference	Yb-B-Ph ₃ PO	Dy-B-Cy ₃ PO
Chemical formula	C ₇₂ H ₅₄ B ₃ YbO ₁₄ P ₂ ·2C ₇ H ₈	C ₇₂ H ₉₀ B ₃ DyO ₁₄ P ₂
Formula Mass	1594.83	1436.30
Temperature (K)	180.0	180.0
Crystal system	triclinic	orthorhombic
Space group	<i>P</i> -1	<i>Pbca</i>
<i>a</i> (Å)	14.0429(8)	22.5723(13)
<i>b</i> (Å)	16.7888(9)	24.4828(17)
<i>c</i> (Å)	18.4141(11)	24.8294(17)
α (°)	79.051(2)	90
β (°)	69.845(2)	90
γ (°)	71.848(2)	90
Unit cell volume (Å ³)	3856.1(4)	13721.5(16)
<i>Z</i>	2	8
ρ_{calc} (g/cm ³)	1.374	1.391
μ / mm ⁻¹	1.319	1.200
<i>F</i> (000)	1626	5960
Radiation	MoK α ($\lambda = 0.71073$)	MoK α ($\lambda = 0.71073$)
Reflections collected	68156	197972
Independent reflections	13507	12655
<i>R</i> _{int}	0.0304	0.1533
GOF on <i>F</i> ²	1.085	1.138
<i>R</i> ₁ ($I \geq 2\sigma(I)$)	0.0261	0.0790
<i>wR</i> ₂ (all data)	0.0656	0.2417
CCDC number	2165283	2165423

Table S3. The CShM's values of the first coordination sphere for **Ln-B-Ph₃PO** and **Dy-B-Cy₃PO**.

Central atom	Coordination Geometry	Dy-B-Ph ₃ PO	Yb-B-Ph ₃ PO
Ln	Octagon (D _{8h})	32.04	31.359
	Heptagonal pyramid (C _{7v})	22.60	22.009
	Hexagonal bipyramid (D _{6h})	0.207	0.577
	Cube (O _h)	8.57	7.381
	Square antiprism (D _{4d})	18.60	15.676
	Triangular dodecahedron (D _{2d})	15.82	12.912
Central atom	Coordination Geometry	Gd-B-Ph ₃ PO	Dy-B-Cy ₃ PO
Ln	Octagon (D _{8h})	31.307	31.264
	Heptagonal pyramid (C _{7v})	22.060	21.681
	Hexagonal bipyramid (D _{6h})	0.488	0.255
	Cube (O _h)	7.501	8.192
	Square antiprism (D _{4d})	16.054	17.815
	Triangular dodecahedron (D _{2d})	13.285	15.070

Table S4. Selected bond distances (\AA) for complexes **Ln-B-Ph₃PO** and **Dy-B-Cy₃PO**.

Dy-B-Ph₃PO	Yb-B-Ph₃PO
Dy1-O1 2.215(3)	Yb1-O1 2.3181(17)
Dy1-O2 2.205(3)	Yb1-O2 2.3331(17)
Dy1-O3 2.3547(16)	Yb1-O3 2.3446(17)
Dy1-O3 ² 2.3547(16)	Yb1-O4 2.1815(18)
Dy1-O3 ³ 2.3546(16)	Yb1-O5 2.3389(17)
Dy1-O4 ¹ 2.3570(16)	Yb1-O6 2.3579(17)
Dy1-O4 ² 2.3570(16)	Yb1-O7 2.3127(18)
Dy1-O4 ³ 2.3570(16)	Yb1-O8 2.1683(18)

Gd-B-Ph₃PO	Dy-B-Cy₃PO
Gd1-O8 2.3859(14)	Dy1-O1 2.215(6)
Gd1-O7 2.3932(14)	Dy1-O2 2.218(6)
Gd1-O5 2.3602(14)	Dy1-O3 2.361(6)
Gd1-O4 2.3709(15)	Dy1-O4 2.360(6)
Gd1-O6 2.3819(15)	Dy1-O5 2.360(6)
Gd1-O1 2.2682(15)	Dy1-O6 2.356(6)
Gd1-O2 2.2439(15)	Dy1-O7 2.366(6)
Gd1-O3 2.3569(15)	Dy1-O8 2.364(6)

Table S5. Selected bond angles ($^{\circ}$) for complexes **Dy-B-Ph₃PO** and **Yb-B-Ph₃PO**.

Dy-B-Ph ₃ PO	Yb-B-Ph ₃ PO
O1 Dy1 O3 90.76(4)	O1 Yb1 O2 64.85(6)
O1 Dy1 O3 ² 90.76(4)	O1 Yb1 O3 172.72(6)
O1 Dy1 O3 ³ 90.76(4)	O1 Yb1 O5 55.73(6)
O1 Dy1 O4 ¹ 90.50(4)	O1 Yb1 O6 120.75(6)
O1 Dy1 O4 ² 90.50(4)	O2 Yb1 O3 119.81(6)
O1 Dy1 O4 ³ 90.50(4)	O2 Yb1 O5 119.91(6)
O2 Dy1 O1 180.0	O2 Yb1 O6 171.95(6)
O2 Dy1 O3 ¹ 89.24(4)	O3 Yb1 O6 55.32(6)
O2 Dy1 O3 ² 89.24(4)	O4 Yb1 O1 86.99(7)
O2 Dy1 O3 ³ 89.24(4)	O4 Yb1 O2 98.15(7)
O2 Dy1 O4 ¹ 89.50(4)	O4 Yb1 O3 86.74(7)
O2 Dy1 O4 ² 89.50(4)	O4 Yb1 O5 87.43(7)
O2 Dy1 O4 ³ 89.50(4)	O4 Yb1 O6 88.20(7)
O3 ¹ Dy1 O3 ² 120	O4 Yb1 O7 85.18(7)
O3 ² Dy1 O3 ³ 120	O5 Yb1 O3 120.23(6)
O3 ¹ Dy1 O3 ³ 120	O5 Yb1 O6 65.07(6)
O3 ¹ Dy1 O4 ¹ 55.30(5)	O7 Yb1 O1 118.19(6)
O3 ² Dy1 O4 ² 55.30(5)	O7 Yb1 O2 55.95(6)
O3 ¹ Dy1 O4 ² 175.14(5)	O7 Yb1 O3 64.92(6)
O3 ² Dy1 O4 ³ 175.14(5)	O7 Yb1 O5 170.75(6)
O3 ³ Dy1 O4 ³ 55.30(5)	O7 Yb1 O6 120.14(6)
O3 ³ Dy1 O4 ¹ 175.14(5)	O8 Yb1 O1 94.69(7)
O3 ¹ Dy1 O4 ³ 64.69(5)	O8 Yb1 O2 83.92(7)
O3 ² Dy1 O4 ¹ 64.69(5)	O8 Yb1 O3 91.48(7)
O3 ³ Dy1 O4 ² 64.69(5)	O8 Yb1 O4 177.76(7)
O4 ¹ Dy1 O4 ² 120	O8 Yb1 O5 92.29(7)
O4 ¹ Dy1 O4 ³ 120	O8 Yb1 O6 89.67(7)
O4 ² Dy1 O4 ³ 120	O8 Yb1 O7 95.31(7)

Table S6. Selected bond angles ($^{\circ}$) for complexes **Gd-B-Ph₃PO** and **Dy-B-Cy₃PO**.

Gd-B-Ph ₃ PO	Dy-B-Cy ₃ PO
O8 Gd1 O7 55.06(5)	O3 Dy1 O8 64.3(2)
O5 Gd1 O8 172.11(5)	O3 Dy1 O7 119.7(2)
O5 Gd1 O7 120.64(5)	O6 Dy1 O3 175.5(2)
O5 Gd1 O4 64.85(5)	O6 Dy1 O5 55.2(2)
O5 Gd1 O6 55.33(5)	O6 Dy1 O8 120.3(2)
O4 Gd1 O8 119.88(5)	O6 Dy1 O4 119.9(2)
O4 Gd1 O7 173.80(5)	O6 Dy1 O7 64.8(2)
O4 Gd1 O6 119.88(5)	O5 Dy1 O3 120.3(2)
O6 Gd1 O8 120.24(5)	O5 Dy1 O8 175.3(2)
O6 Gd1 O7 65.37(5)	O5 Dy1 O4 64.8(2)
O1 Gd1 O8 85.88(5)	O5 Dy1 O7 119.9(2)
O1 Gd1 O7 86.87(5)	O2 Dy1 O3 91.8(2)
O1 Gd1 O5 87.28(6)	O2 Dy1 O6 88.0(2)
O1 Gd1 O4 96.55(5)	O2 Dy1 O5 86.2(2)
O1 Gd1 O6 86.65(6)	O2 Dy1 O8 92.5(2)
O1 Gd1 O3 84.67(6)	O2 Dy1 O4 90.2(2)
O2 Gd1 O8 91.70(6)	O2 Dy1 O7 88.7(2)
O2 Gd1 O7 91.27(6)	O8 Dy1 O7 55.5(2)
O2 Gd1 O5 95.09(6)	O4 Dy1 O3 55.5(2)
O2 Gd1 O4 85.15(6)	O4 Dy1 O8 119.8(2)
O2 Gd1 O6 94.08(6)	O4 Dy1 O7 175.1(2)
O2 Gd1 O1 177.51(6)	O1 Dy1 O3 93.2(2)
O2 Gd1 O3 94.85(6)	O1 Dy1 O6 87.0(2)
O3 Gd1 O8 65.09(5)	O1 Dy1 O5 91.3(2)
O3 Gd1 O7 119.97(5)	O1 Dy1 O2 175.0(2)
O3 Gd1 O5 118.14(5)	O1 Dy1 O8 89.8(2)
O3 Gd1 O4 55.49(5)	O1 Dy1 O4 92.6(2)
O3 Gd1 O6 169.46(5)	O1 Dy1 O7 88.9(3)

4. TGA and magnetic measurements

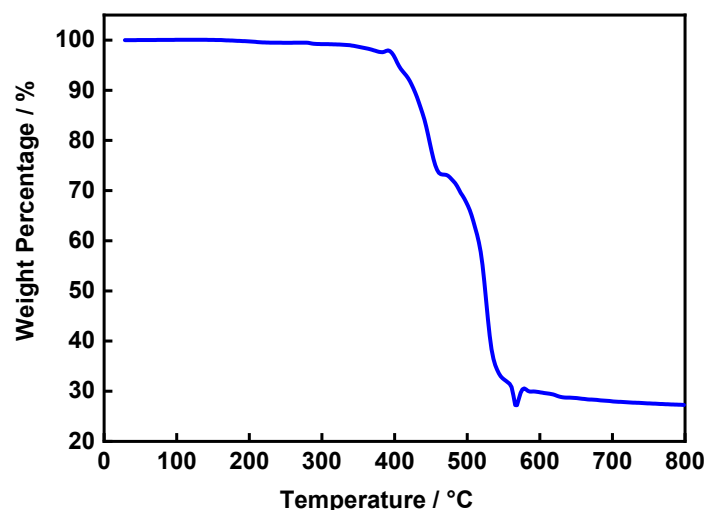


Fig. S2. Thermogravimetric analysis of **Dy-B-Ph₃PO**.

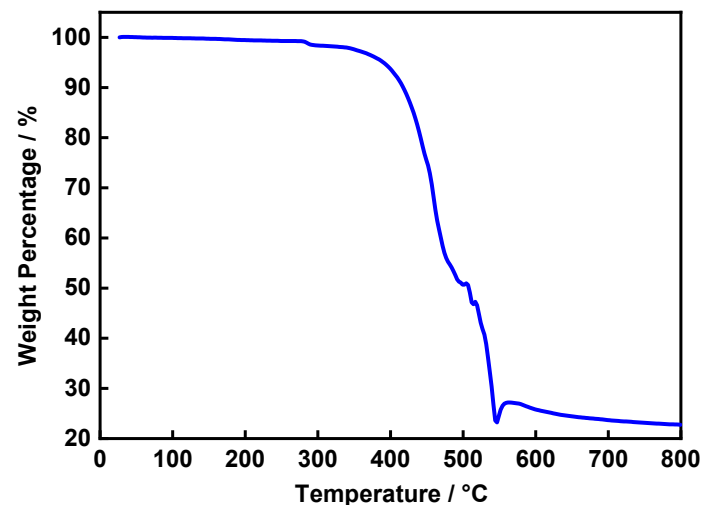


Fig. S3. Thermogravimetric analysis of **Dy-B-Cy₃PO**.

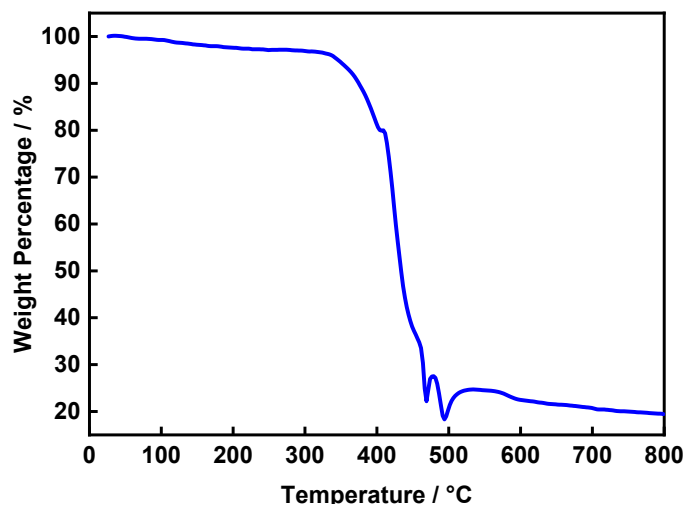


Fig. S4. Thermogravimetric analysis of Yb-B-AnPh₃PO.

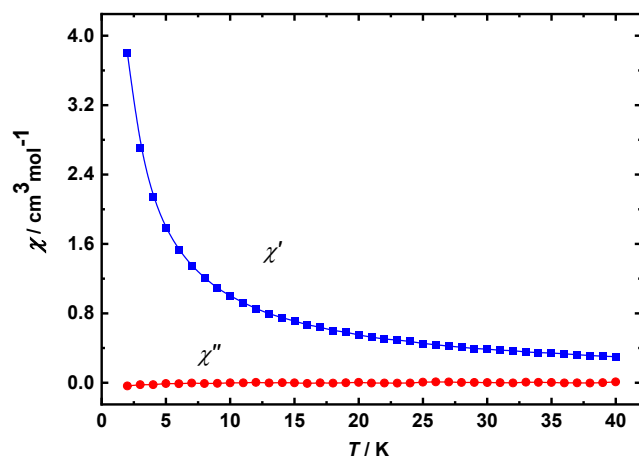


Fig. S5. Temperature dependence of ac susceptibility for Dy-B-Ph₃PO in zero dc field at the frequency of 997 Hz.

5. Photophysical Properties

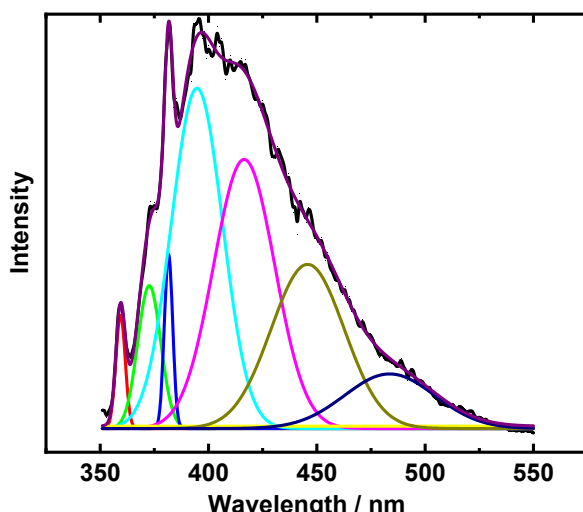


Fig. S6. Phosphorescence spectrum of **Gd-B-Ph₃PO** collected in the solid state under excitation at 290 nm (black line, 77 K) and its Gaussian decomposition (colored traces).

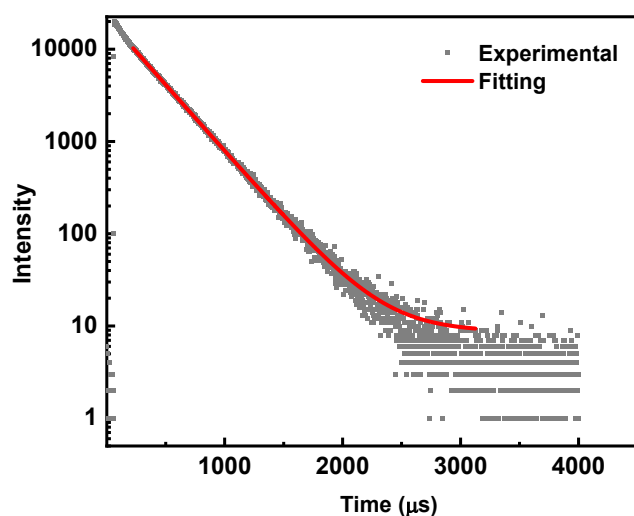


Fig. S7. Decay curves of **Dy-B-Ph₃PO** in CDCl₃ solution ($c = 1.5 \times 10^{-5}$ mol/L) at room temperature.

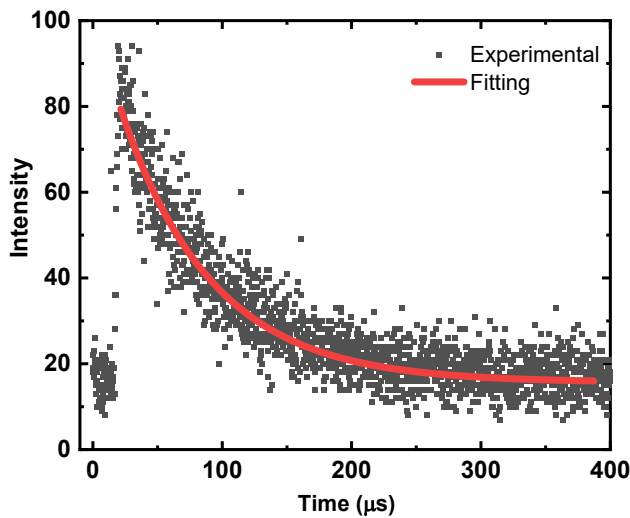


Fig. S8. Decay curves of **Yb-B-Ph₃PO** in CDCl₃ solution ($c = 1.5 \times 10^{-5}$ mol/L) at room temperature.

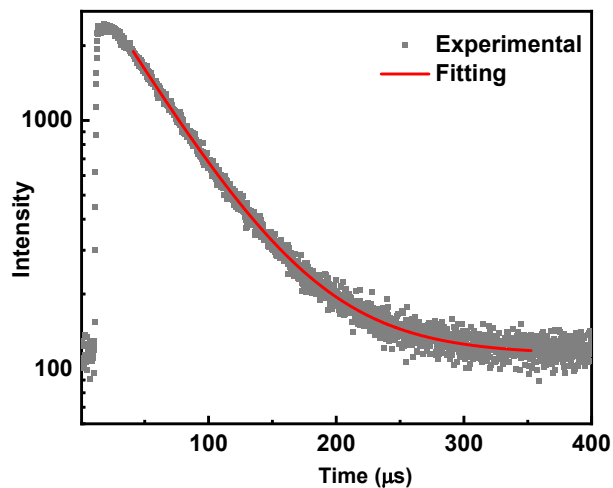


Fig. S9. Decay curves of **Yb-B-AnPh₃PO** in the solid state at room temperature.

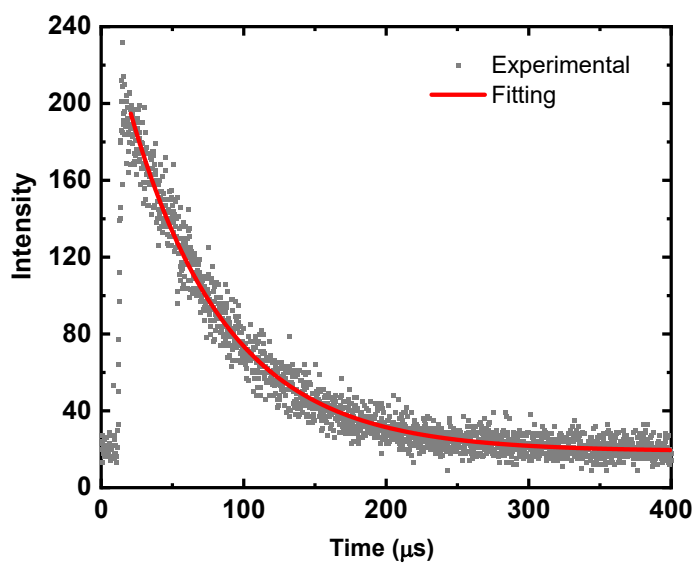


Fig. S10. Decay curves of **Yb-B-AnPh₃PO** in CHCl₃ solution ($c = 1.5 \times 10^{-5}$ mol/L) at room temperature.

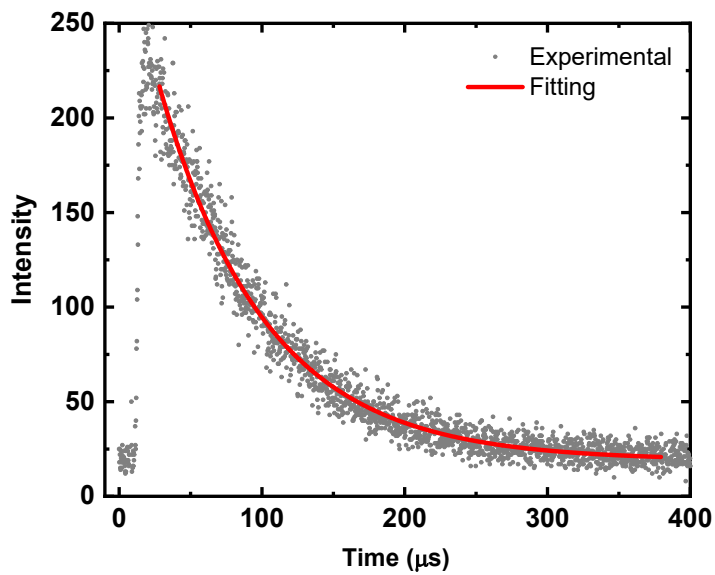


Fig. S11. Decay curves of **Yb-B-AnPh₃PO** in CDCl₃ solution ($c = 1.5 \times 10^{-5}$ mol/L) at room temperature.

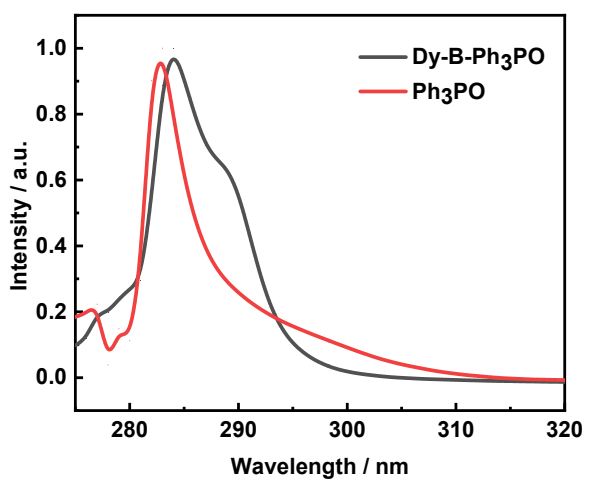


Fig. S12. Absorption spectra of Ph₃PO and **Dy-B-Ph₃PO** in THF ($c = 1.5 \times 10^{-5}$ mol/L mol/L) at room temperature.

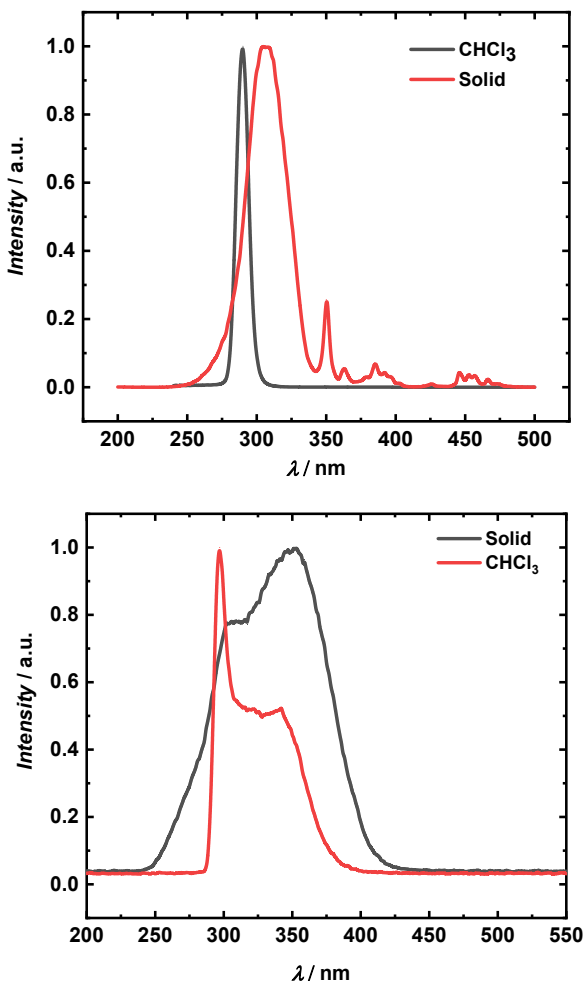


Fig. S13. Excitation spectra of **Dy-B-Ph₃PO** (top) and **Yb-B-Ph₃PO** (bottom) in solid state and CHCl₃ solution under monitoring the main f-f transitions of Dy³⁺ ion at 580 nm and Yb³⁺ ion at 980 nm at room temperature.

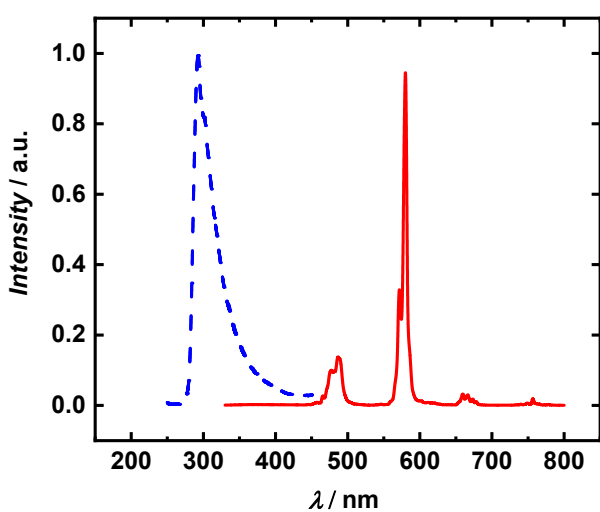


Fig. S14. Normalized emission spectra of Ph₃PO and **Dy-B-Ph₃PO** in the solid state under the excitation at 240 nm and 300 nm, respectively, at room temperature.

Table S7. Photophysical data for Dy(III) complexes at room temperature reported in literature.

Complex	τ_{obs} (μs)	Φ_{overall} (%)	state	ref.
Dy(PPI) ₃ (DPEPO)	33	12	solid	[6]
[DyR(+)-BnMe22IAM]	18	1.3	CH ₃ OH	[7]
[DyGa ₄ (shi) ₄ (C ₆ H ₅ CO ₂) ₄ (C ₅ H ₅ N) (CH ₃ OH)]	21	1.2	solid	[8]
[(AsW ₉ O ₃₃) ₇ Dy ₇ W ₈ O ₂₁ (H ₂ O) ₁₇ (μ ₃ -OH)(OH)]	41.5	-	solid	[9]
{[Dy ₂ (bpda) ₃ (H ₂ O) ₃] ₄ ·2H ₂ O}	8	1.24	solid	[10]
[LnGa ₄ (shi) ₄ (H ₂ shi) ₂ (py) ₄ (NO ₃)](py) ₂	3.36	0.22	solid	[11]
{[Ln(H ₂ BIDC)(HBIDC)(H ₂ O) ₃]·3H ₂ O}n	7.63	-	solid	[12]

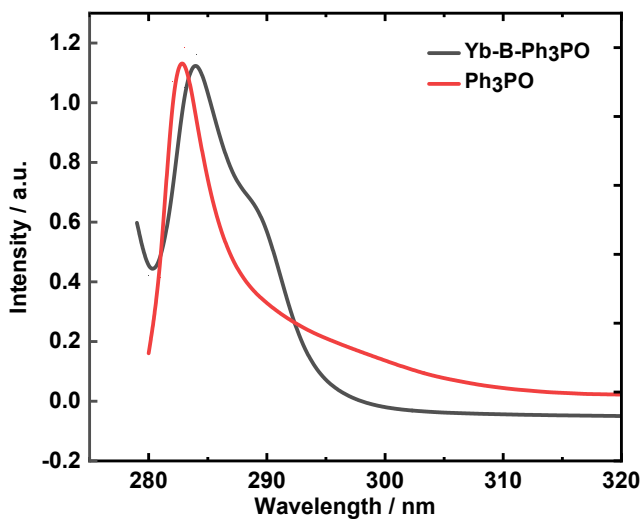


Fig. S15. Absorption spectra of **Ph₃PO** and **Yb-B-Ph₃PO** in **CHCl₃** ($c = 1.5 \times 10^{-5}$ mol/L) at room temperature.

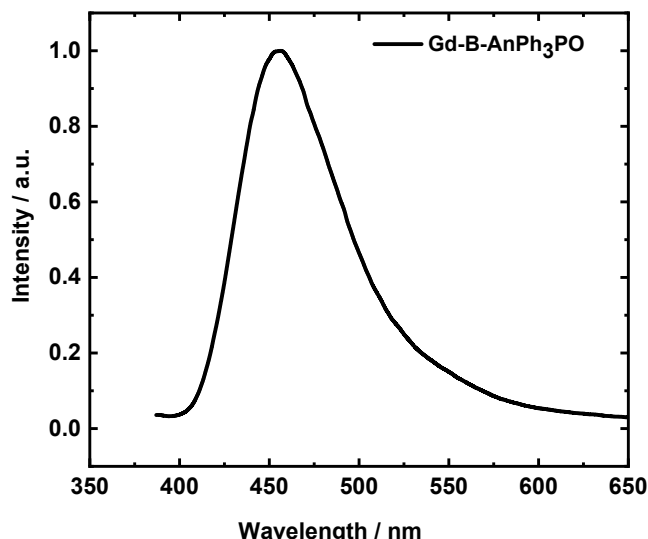


Fig. S16. Phosphorescence spectrum of **Gd-B-AnPh₃PO** collected in the solid state under excitation at 360 nm at 77 K.

6. Living Cell Imaging

Cytotoxicity evaluation in vitro. CCK-8 assay was carried out to evaluate the dark toxicity and phototoxicity of **Yb-B-AnPh₃PO**. HeLa cells were seeded into 96-well plates at the density of 1×10^4 per well and incubated at 37 °C for 24 h. After removal of the medium and rinsing with PBS, HeLa were pretreated with compound **Yb-B-AnPh₃PO** (final concentration contains 0, 5, 10, 15, 20 or 25 μM), respectively. One plate was kept in the dark for studying dark toxicity, and another plate was irradiated using the 400-700 nm laser at a power of 10 mW cm⁻² for 10 min. All group cells were incubated for another 24 h, the cell viability was detected by added of Cell Counting Kit-8 (CCK-8, 10 μL), and the absorbance at a wavelength of 450 nm of each well was measured using a 96-well plate reader. The cell viability was then determined via the following equation: cell viability (%) = (mean of abs. value of treatment group/mean abs. value of control) × 100%.

Fluorescence imaging of Yb-B-AnPh₃PO in live HeLa cell. **Yb-B-AnPh₃PO** was diluted with DMEM to work concentration (10 μM). **Yb-B-AnPh₃PO** solution was added to the Hela cells and incubating at 37 °C for 3 h, then washed twice with PBS buffer (1×, pH = 7.4), and kept in fresh FBS-free DMEM for observation under a microscope (Excitation: $\lambda = 375$ nm. Emission: 776 nm long pass filter + 980nm long pass filter).

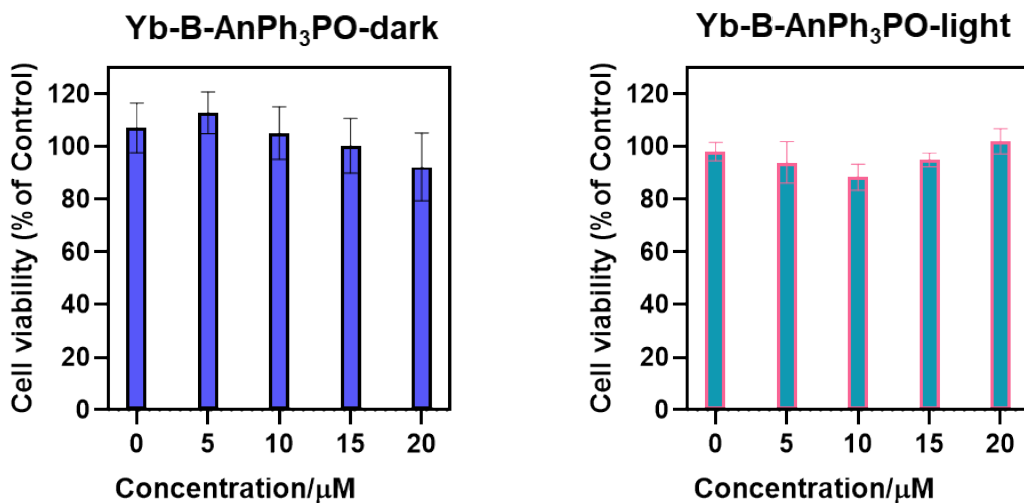


Fig. S17. Plots of results of the cytotoxicity test for **Yb-B-AnPh₃PO** incubated with HeLa cells during 24 h.

7. References:

1. W. Huang, B. M. Upton, S. I. Khan and P. L. Diaconescu, *Organometallics*, 2013, **32**, 1379-1386.
2. P. Zhang, L. Zhang, C. Wang, S. Xue, S.-Y. Lin and J. Tang, *J. Am. Chem. Soc.*, 2014, **136**, 4484-4487.
3. Y. Yu, L. Ma, Z. Feng, B. Liu, H. Zhou, H. Qin, H. Li, J. Song, G. Zhou and Z. Wu, *J. Mater. Chem. C*, 2019, **7**, 5604-5614.
4. O. V. Dolomanov, L. J. Bourhis, R. J. Gildea, J. A. K. Howard and H. Puschmann, *J. Appl. Crystallogr.*, 2009, **42**, 339-341.
5. E. A. Boudreux and L. N. Mulay, John Wiley & Sons, New York, 1976.
6. S. Biju, N. Gopakumar, J. C. G. Bünzli, R. Scopelliti, H. K. Kim and M. L. P. Reddy, *Inorg. Chem.*, 2013, **52**, 8750-8758.
7. S. Petoud, G. Muller, E. G. Moore, J. Xu, J. Sokolnicki, J. P. Riehl, U. N. Le, S. M. Cohen and K. N. Raymond, *J. Am. Chem. Soc.*, 2007, **129**, 77-83.
8. C. Y. Chow, S. V. Eliseeva, E. R. Trivedi, T. N. Nguyen, J. W. Kampf, S. Petoud and V. L. Pecoraro, *J. Am. Chem. Soc.*, 2016, **138**, 5100-5109.
9. J. Xiong, Z.-X. Yang, P. Ma, D. Lin, Q. Zheng and Y. Huo, *Inorg. Chem.*, 2021, **60**, 7519-7526.
10. R.-f. Li, R.-h. Li, X.-f. Liu, X.-h. Chang and X. Feng, *RSC Adv.*, 2020, **10**, 6192-6199.
11. T. N. Nguyen, S. V. Eliseeva, C. Y. Chow, J. W. Kampf, S. Petoud and V. L. Pecoraro, *Inorg. Chem. Front.*, 2020, **7**, 1553-1563.
12. P. Wang, R.-Q. Fan, Y.-L. Yang, X.-R. Liu, P. Xiao, X.-Y. Li, W. Hasi and W.-W. Cao, *CrystEngComm*, 2013, **15**, 4489-4506.